

## **Versatile Bandpass Filters with Wide Frequency Tunability**

### **Part I**

#### **Version 2.0**

James A Crawford

---

### **Synopsis**

*Classical LC filter design is becoming increasingly rare in much of the RF design community. This is in part due to the domination of direct-conversion in up- and down-converters and the widespread availability of excellent off-the-shelf filter components (e.g., SAW filters).*

*Whether the occasion be discrete design or on-chip integrated design, the need for tunable bandpass filters still arises. In Part I of this article, single-pole bandpass filter design is considered for situations where passband flatness is not overly demanding but insertion loss may be a critical requirement. Part II of this article looks at the design of 2<sup>nd</sup>-order tunable bandpass filters which may prove indispensable in some circumstances.*

*This paper contains both tutorial as well as more academic material, and should be sufficient to form a starting point for real hardware design efforts.*

## 1 Why Tunable Filters?

Tunable filters can be indispensable when selectivity requirements would otherwise translate into a prohibitively large number of fixed filters in a switched-filter bank. To illustrate this point, consider a situation where the desired signal frequency ranges from  $f_{sigmin} = 100$  MHz to  $f_{sigmax} = 200$  MHz and a specified amount of stopband attenuation must be applied to the 2<sup>nd</sup> (and higher) harmonic of the signal thereby dictating a stopband which spans from 200 MHz to 400 MHz for the 2<sup>nd</sup> harmonic.

If the switched bank of filters consists of strictly Butterworth lowpass filters<sup>1</sup>, the stopband attenuation for a specific filter is given by

$$A_{stop}(f) = 10 \log_{10} \left[ 1 + \left( \frac{f}{f_c} \right)^{2N} \right] \text{ dB} \quad (1)$$

where  $f_c$  is the  $-3$  dB corner frequency of the filter and  $N$  is the order of the filter. For a specified amount of attenuation in the frequency stopband, (1) can be rewritten as

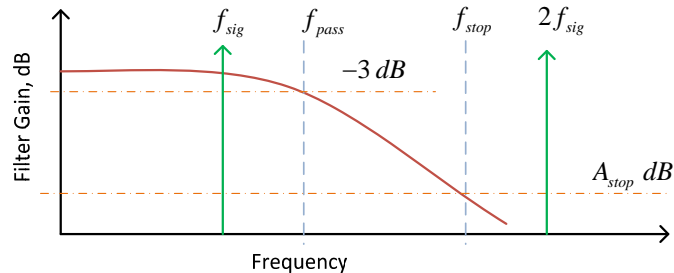
$$\frac{f_{stop}}{f_{pass}} \leq \left[ 10^{0.1A_{stop}} - 1 \right]^{1/(2N)} \quad (2)$$

where the stopband attenuation requirement is given by  $A_{stop}$ . These filter quantities are related as shown in Figure 1. In order to adequately suppress the second harmonic of the signal, it must be true that

$$2f_{sig\_min} \geq f_{stop} \quad (3)$$

Consequently, the useable frequency range for the  $k^{\text{th}}$  lowpass filter in the filter bank is given by

$$\left[ \frac{f_{stop_k}}{2}, f_{pass_k} \right] \quad (4)$$



**Figure 1** Key frequencies as they pertain to a single Butterworth lowpass filter

<sup>1</sup> Normally, elliptic or Chebyshev filters would be used for greater economy, but the underlying arguments are the same.

The relationship between  $f_{stop}$  and  $f_{pass}$  for the  $k^{th}$  filter in (4) is dictated by the minimum stopband attenuation requirement  $A_{stop}$  by way of (2).

In this present context, it has been assumed that the output signal's amplitude can vary up to  $-3$  dB due to the roll-off of the Butterworth filters at  $f_{pass}$ . If less signal level variation is required, more Butterworth filters will be required in the filter bank or a different filter family (e.g., elliptical) will have to be adopted.

It will prove very helpful to compute the filter shape factor<sup>2</sup> for the Butterworth lowpass filter family based upon (2) as done in Table 1. The smaller the shape factor in Table 1, the more selective the filter is. In order to be useful for 2<sup>nd</sup> harmonic suppression, the shape factor must be less than 2.

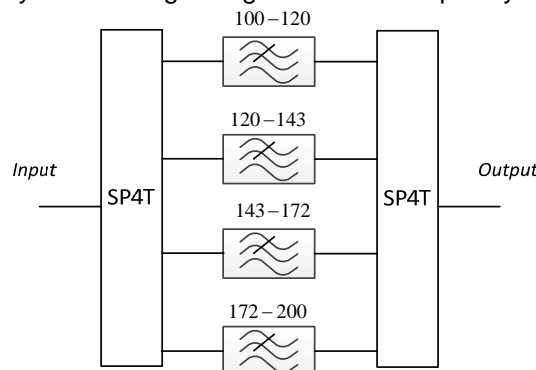
**Table 1** Butterworth Lowpass Filter Shape Factors

Filter Order	Minimum Stopband Attenuation, dB				
	10	20	30	40	50
1	3	9.95	31.61	–	–
3	1.44	2.15	3.16	4.64	6.81
5	1.25	1.58	2.00	2.51	3.16
7	1.17	1.39	1.64	1.93	2.28
9	1.13	1.29	1.47	1.67	1.90

For the given example, assume that the minimum stopband attenuation requirement is 40 dB. In order to have a reasonably sized filter bank, the shape factor must be as small as possible compared to 2. For this 40 dB example, a 9<sup>th</sup>-order Butterworth lowpass has an associated shape factor of 1.67 from Table 1. The corner frequencies for the constituent lowpass filters are given by

$$f_c(k) = \frac{2f_c(k-1)}{shapefactor} \quad \text{for } k \geq 1 \tag{5}$$

where  $f_c(0) = f_{sigmin}$ . Consequently, the corner frequencies for this example are {119.8, 143.4, 171.8, 205.8 } MHz and a minimum of four 9<sup>th</sup>-order Butterworth lowpass filters are required plus a supporting switch fabric as shown in Figure 2. This represents a fair amount of circuit complexity for covering a single octave in frequency.



**Figure 2** Idealized switched filter bank using four 9<sup>th</sup>-order Butterworth lowpass filters

Smaller shape factors can be realized using Chebyshev or elliptical filters, but the computations given by (5) would still apply.

<sup>2</sup> The shape factor for a lowpass filter is given by  $f_{stop} / f_{pass}$ . In [1], this same quantity is referred to as the filter's steepness factor.

### Filter Banks Using Bandpass Filters

Alternatively, a switched bank of Butterworth bandpass filters can be considered. The number of filters required will generally be less if bandpass filters are used, but the circuit complexity still remains fairly high.

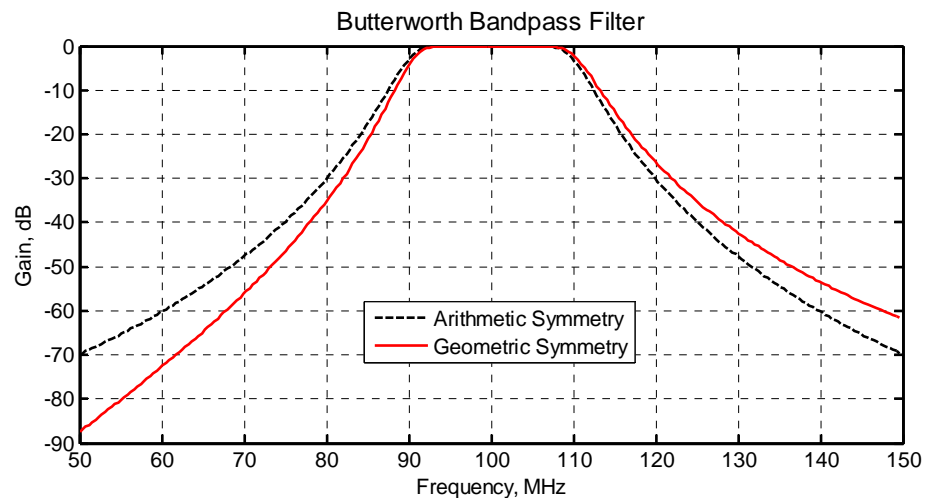
In the Butterworth bandpass filter case, (1) still applies provided that the quantity in parentheses is replaced by the lowpass-to-bandpass frequency transformation which is given by<sup>3</sup>

$$u(f) = \frac{f^2 - f_o^2}{f B} \quad (6)$$

where  $f_o$  is the center frequency of the filter involved and  $B$  is the filter's ripple-bandwidth ( $-3$  dB bandwidth in the case of Butterworth bandpass filters). This is not the only means to create a bandpass filter shape, but it is very convenient for the discussions underway here. Bandpass filters of this form exhibit geometric frequency symmetry<sup>4</sup> about the center frequency, but arithmetic symmetry can be assumed with little loss of precision so long as the filter's percentage bandwidth remains small (typically  $< 20\%$ ). The frequencies corresponding to the filter's  $-3$  dB edges occur for  $u(f) = \pm 1$ , namely

$$f_{\text{passband-edges}} = f_o \sqrt{1 + \left(\frac{B}{2f_o}\right)^2} \pm \frac{B}{2} \quad (7)$$

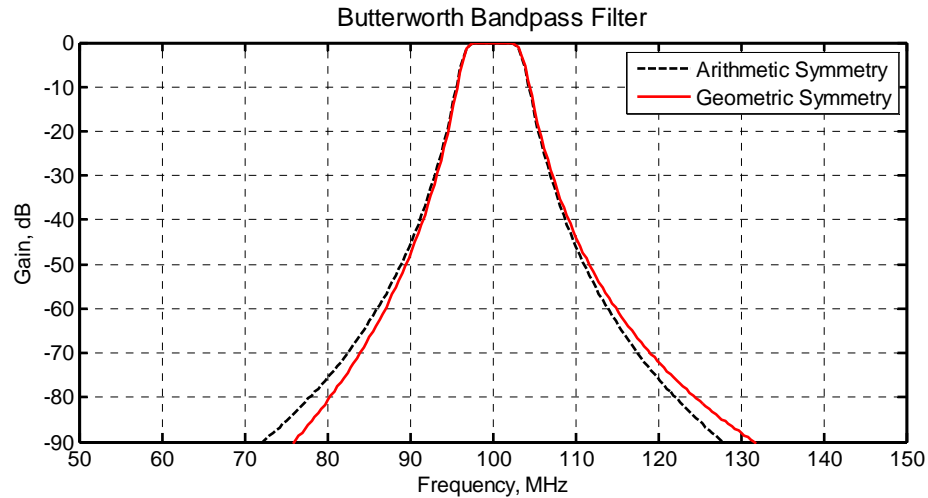
To illustrate the difference between arithmetic and geometric symmetry, the gain characteristics for a 5<sup>th</sup>-order Butterworth bandpass filter having a 20% bandwidth are shown in Figure 3. As the percentage bandwidth gets smaller, the two frequency responses becomes increasingly the same as shown in Figure 4.



**Figure 3** Frequency responses for  $N = 5$  Butterworth bandpass filter having 20 MHz  $-3$  dB bandwidth exhibiting (i) arithmetic symmetry and (ii) geometric symmetry

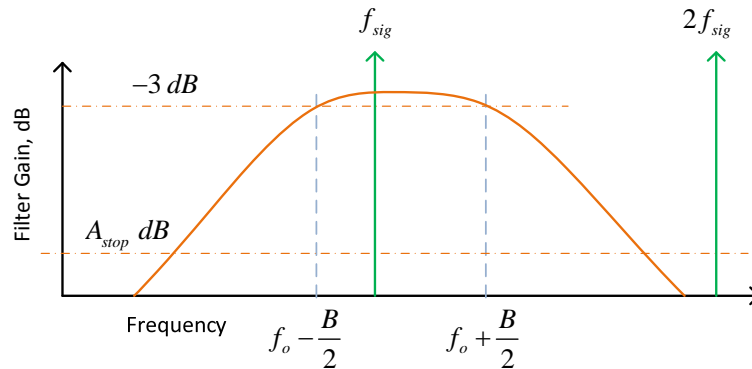
<sup>3</sup> See Chapter 5 of [1].

<sup>4</sup> See Chapter 5 of [1].



**Figure 4** 5<sup>th</sup> order Butterworth bandpass filter with 7% fractional bandwidth illustrating the similarities between the arithmetic symmetric response and geometric symmetric response for smaller percentage bandwidth cases

Returning now to (7), notice that the  $-3$  dB bandwidth of the filter is precisely  $B$  Hertz whereas the center frequency of the filter is shifted slightly higher than  $f_o$ . So long as the filter’s percentage bandwidth<sup>5</sup> remains less than 20%, the center frequency shift will be less than 0.5%.



**Figure 5** Useable frequency range for an individual Butterworth bandpass filter

The useable frequency range for an individual Butterworth bandpass filter can be determined by making use of Figure 5. At the low-end of the useable frequency range, the allowable signal frequency equals approximately<sup>6</sup>  $f_o - B/2$  and the stopband attenuation at the 2<sup>nd</sup> harmonic of this frequency must meet the requirement  $A_{stop}$  (dB). Provided this is true and the stopband behavior is monotonic, the upper limit for the useable frequency range is simply given by  $f_o + B/2$ . The useable frequency range is then dictated by the filter’s shape factor as it pertains to the stopband attenuation requirement  $A_{stop}$  and the lower frequency limit  $f_o - B/2$ .

Referring to Figure 6, the passband width of the filter is  $B$  whereas the stopband width as it pertains to the 2<sup>nd</sup> harmonic of  $f_o - B/2$  is  $2(f_o - B)$ . The corresponding

<sup>5</sup> Percentage bandwidth is defined here as  $B / f_o$ .  
<sup>6</sup> Making use of (7) while ignoring the quadratic term.

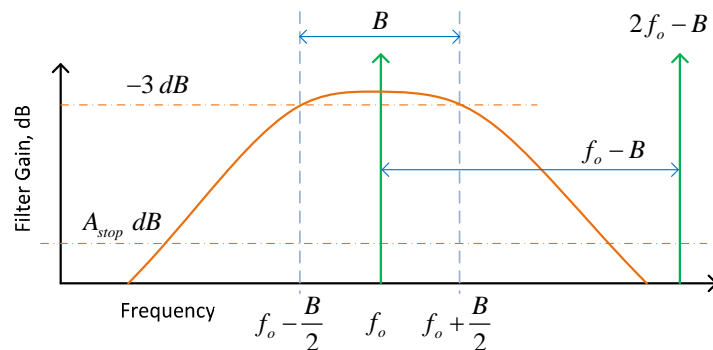
shape factor for the filter is then given by the ratio of the stopband frequency width to the passband frequency width as

$$\text{shapefactor}_{bpf} = \frac{2(f_o - B)}{B} = 2\left(\frac{f_o}{B} - 1\right) \quad (8)$$

Note that a filter's shape factor may be defined differently in other situations. The shape factor given by (8) pertains only to the 2<sup>nd</sup> harmonic situation of interest here. The quantity  $B / f_o$  should also be recognized as the fractional bandwidth of the filter.

### Improved Shape Factor Precision

The result given by (8) is the commonly used value for the filter's shape factor, but the exact shape factor must generally be calculated using (6) because the true bandpass filter exhibits geometric frequency symmetry rather than arithmetic symmetry.



**Figure 6** Shape factor for a Butterworth bandpass filter

Equation (6) should be thought of as a straight forward frequency transformation. It has already been stated that the transformed frequency value at the passband edges is (very nearly)  $\pm 1$ . The transformed frequency value at the lowest 2<sup>nd</sup> harmonic value ( $2f_o - B$ ) is given by

$$\gamma_+ = u \left[ 2 \left( f_o - \frac{B}{2} \right) \right] \quad (9)$$

The transformed frequency value in the lower frequency stopband region is similarly given by

$$\gamma_- = u [B] \quad (10)$$

When the bandpass filter is constructed based upon (6), it turns out that the upper stopband attenuation characteristic is a bit more lazy than the lower stopband characteristic. Consequently, it is always true that  $|\gamma_-| > |\gamma_+|$ . For example, if  $f_o = 100$  MHz and  $B = 10$  MHz,  $\gamma_+ \cong 13.737$  whereas  $\gamma_- \cong -99$ . This is a result of the underlying geometric symmetry of the filter's attenuation characteristic rather than it being arithmetic symmetric as discussed earlier regarding Figure 3.

It is very convenient to define a filter shape factor based upon the transformed frequency relationship. To this end, the transformed frequency passband width is simply 2. Since the primary interest here pertains to suppressing frequency harmonics, the

transformed frequency stopband width will be taken to be  $2\gamma_+$ . The filter's shape factor in terms of the transformed frequency quantities is then simply given by  $2\gamma_+ / 2 = \gamma_+$ . Based upon this result along with (1) and (6), the associated stopband attenuation is given by

$$A_{stop} = 10 \log_{10} \left[ 1 + (\gamma_+)^{2N} \right] \quad (11)$$

Continuing on from (9), there is no need to carry the "+" subscript since only the upper stopband will be of interest from this point on. Equation (9) can be expanded to give

$$(1 + \gamma)B^2 - 2f_o(2 + \gamma)B + 3f_o^2 = 0 \quad (12)$$

This is a simple quadratic equation which can be solved for the bandwidth  $B$  given assumed values for the filter's center frequency  $f_o$  with the shape factor  $\gamma$  again dictated by Table 1 for a given amount of required stopband attenuation. The solution can be expressed in terms of the fractional bandwidth ( $\chi$ ) by dividing (12) by  $f_o^2$  as

$$(1 + \gamma)\chi^2 - 2(2 + \gamma)\chi + 3 = 0 \quad (13)$$

which leads to

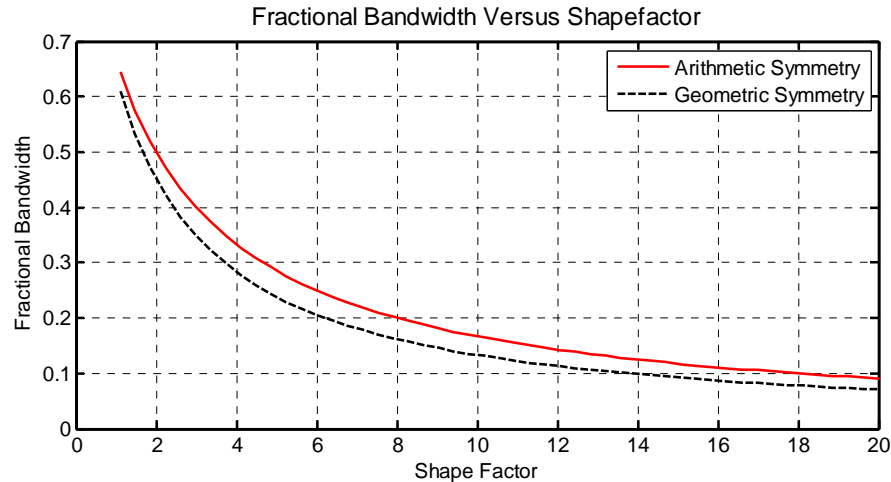
$$\chi = \frac{2 + \gamma - \sqrt{\gamma^2 + \gamma + 1}}{1 + \gamma} \quad (14)$$

It is worthwhile comparing this exact result with the approximate result from (8). Equation (8) can be recast in terms of fractional bandwidth as

$$\chi = \frac{2}{2 + \text{shapefactor}_{bpf}} \quad (15)$$

The approximate relationship between filter shape factor and fractional bandwidth is given by (8) (assuming arithmetic filter symmetry) whereas the exact result is given by (14). These results are shown plotted together in Figure 7. The approximate result is always too optimistic in terms of the allowed filter passband width versus the exact result. In actual usage, the filter's true frequency response should be used to determine how many bandpass filters are required in the filter bank. Even so, (14) is helpful for estimating purposes.

Returning to the same example case with the desired frequency range spanning from 100 MHz to 200 MHz and the need to suppress all 2<sup>nd</sup> harmonic (and higher) terms by at least 40 dB, it would be attractive if the bandpass filter bank only required two switched filters. Based upon geometric symmetry arguments, this could be done with one filter's passband covering 100 MHz to 141 MHz, and the second filter covering 141 MHz to 200 MHz, each representing a fractional bandwidth of about 35%. Equation (15)



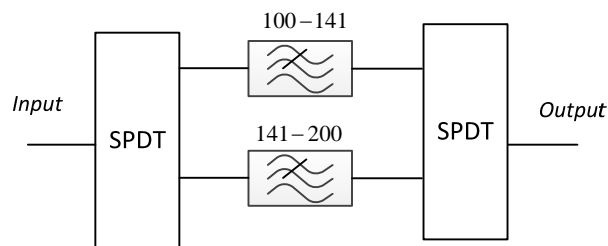
**Figure 7** Fractional bandwidth versus Butterworth bandpass filter shape factor assuming (i) arithmetic symmetry and (ii) geometric symmetry

predicts that  $shapefactor_{bpf} < 3.71$  is required. Equation (13) can be used to express the exact shape factor  $\gamma$  in terms of  $\chi$  as

$$\gamma = \frac{4\chi - \chi^2 - 3}{\chi^2 - 2\chi} \tag{16}$$

thereby predicted a required shape factor  $\gamma \leq 2.98$ . Limiting design considerations to odd-ordered Butterworth bandpass filters, Table 1 shows that 5<sup>th</sup>-order bandpass filters will suffice for the 40 dB stopband attenuation requirement since  $2.51 < 2.98$ .

Rather than require four 9<sup>th</sup>-order Butterworth lowpass filters, a filter bank using only two 5<sup>th</sup>-order Butterworth bandpass filters should achieve the same end result as shown in Figure 8. In Part II of this paper, however, it will be shown that a single  $N = 2$  tunable bandpass filter will deliver the same performance as well which would be a further reduction in hardware complexity as well as cost.

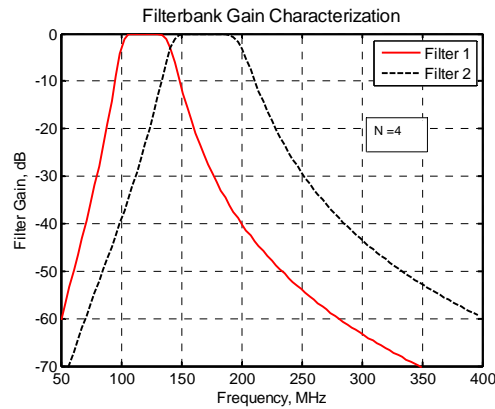


**Figure 8** Bandpass filter bank solution using 5<sup>th</sup>-order Butterworth bandpass filters with frequency responses for 4<sup>th</sup>-order and 5<sup>th</sup>-order bandpass filters shown in Figure 9 and Figure 10

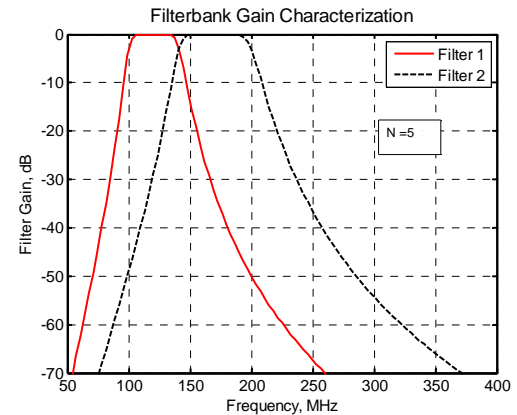
In general, it is possible to conclude:

- A filter bank using only lowpass filters results in the greatest hardware complexity
- A filter bank using only bandpass filters offers a marked improvement over the lowpass filter bank in hardware complexity
- Tunable bandpass filters offer the greatest reduction in hardware complexity.





**Figure 9** Filter bank of Figure 8 using 4<sup>th</sup>-order Butterworth bandpass filters successfully



**Figure 10** Filter bank of Figure 8 using 5<sup>th</sup>-order Butterworth bandpass filters achieves the 40 dB stopband requirement with margin to spare

### Necessary Caveats

Tunable bandpass filters are not always the answer, however. For example,

- Switched lowpass filter banks are generally required in high power applications because filter insertion loss must be kept as low as possible. Inductor currents within bandpass filters typically scale with the filter-Q value which can make inductor heating and even arcing genuine concerns.
- In ultra-low noise figure applications that require front-end filtering, lowpass LC filters will generally have less impact on noise figure than bandpass LC filters.

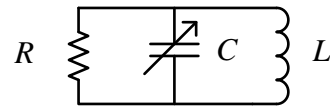
## 1.1 Tunable Bandpass Filter Assumptions and Guidelines

In the traditional LC filter designs considered in this paper, the only physical components available are resistors, capacitors, and inductors. Generally speaking, it is true that:

- Inductors are generally larger than capacitors, especially at lower frequencies.
- Inductors are almost always more expensive than capacitors by a substantial margin.
- Inductors exhibit unwanted magnetic coupling if they are situated too close to each other.
- Inductor Q's are generally worse than capacitor Q's thereby largely dictating filter insertion loss.
- Banks of switched inductors are usually hampered by size, coupling issues, and cost.
- Tunable inductors are generally not available whereas tunable capacitors are available in the form of varactor diodes.
- If one capacitor is adjusted versus frequency, all capacitors in the filter must generally be adjusted.
- Ideal L's and C's are assumed.
- Input and output port impedances will be assumed equal and constant; typically 50Ω.

Given these points, it is desirable to (i) only use switched capacitors or varactors for the tunable elements, and (ii) the number of inductors within a filter should be kept to a minimum.

The impedance level within a filter changes as the filter's center frequency is changed. If this issue is not also dealt with, problems with insertion loss and selectivity will normally come into play. Consider the simple RLC circuit shown in Figure 11 having an adjustable capacitor for changing the resonant frequency. The resonant frequency is given by



**Figure 11** Parallel RLC circuit with adjustable capacitor

$$\omega_o = \frac{1}{\sqrt{LC}} \quad (17)$$

Since only the capacitance is adjustable, the resonant frequency is inversely proportional to  $\sqrt{C}$  so a 2:1 change in frequency will require a 4:1 change in capacitance. The quality factor  $Q$  of the resonator is given by

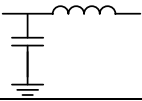

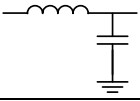


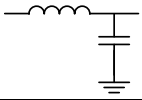
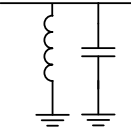
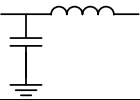


$$Q = \frac{R}{L2\pi f} = \frac{1}{f} \frac{R}{2\pi L} \quad (18)$$

and is inversely proportional to the center frequency  $f$  which is generally undesirable. In order to have a constant- $Q$  resonator, the effective  $R$  must increase linearly with frequency. If the filter bandwidth is to remain constant with  $f$ , the filter  $Q$  must increase linearly with  $f$  which means that the effective  $R$  must increase with  $f^2$ . These and other factors come into play when designing a tunable bandpass filter.

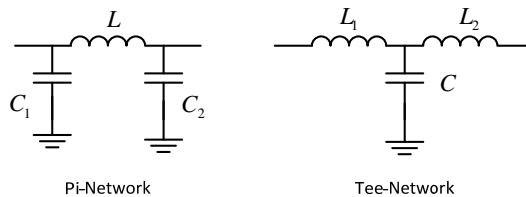
## 2 Getting Started

First-order LC bandpass filters based upon the general construct of cascading an input matching section, LC resonator, and output matching section are considered in this paper as suggested by Table 2. Other input and output matching sections are possible (e.g., all-capacitor L, all-inductor L), but the focus will be kept on minimum-inductor topologies and those exhibiting the best likely performance.

**Table 2** First-Order LC Bandpass Filter Constructs Where An Entity From Each Column is Cascaded

Input Matching	Resonator	Output Matching	
			
			
			
			

The pi- and tee-networks shown in Figure 12 can transform any  $R + jX$  impedance to any other  $R' + jX'$  impedance at a specific frequency. The input and output L-matching networks shown in Table 2 are not as flexible, however. Understanding their limitations is key to understanding how they should be selected in filter design.



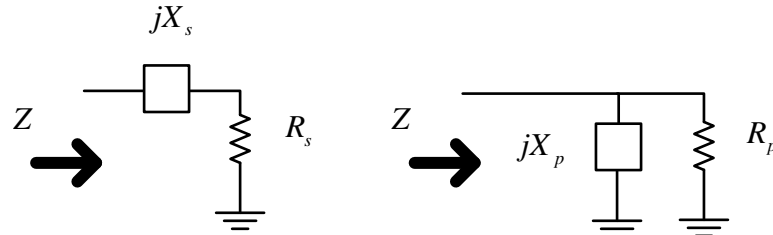
**Figure 12** pi-network and tee-network for impedance matching

Take for instance the simple case in Figure 13 which entails inserting a reactance (capacitive or inductive)  $jX_s$  in series with a load  $R_s$ . The series and parallel networks are equivalent at a specific frequency provided that

$$\begin{aligned}
 R_p &= R_s (1 + Q_s^2) \\
 X_p &= X_s \left( 1 + \frac{1}{Q_s^2} \right)
 \end{aligned}
 \tag{19}$$

where  $Q_s = |X_s| / R_s$ . Note that it is always true that  $R_p > R_s$  so the insertion of a series reactance is used to increase the real value of the impedance at a specific frequency.

Insertion of a series reactance is used to step-up the real impedance level.



**Figure 13** Equivalent series and parallel networks at a specific frequency

The converse is also true from Figure 13 where the inclusion of a shunt reactance  $X_p$  reduces the real impedance value at a specific frequency since

$$R_s = \frac{R_p}{1 + Q_p^2}$$

$$X_s = \frac{X_p}{1 + \left(\frac{1}{Q_p}\right)^2} \quad (20)$$

where  $Q_p = R_p / |X_p|$

Insertion of a parallel reactance is used to step-down the real impedance level.

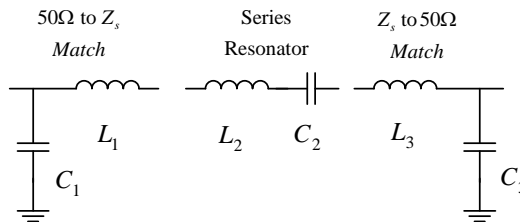
Since equally-terminated filters will be assumed in this paper, stepping down the source impedance using an L-network will require stepping up the output impedance of the filter to match the load impedance. Similarly, if the source impedance is stepped up using an L-network, the output impedance of the filter must be stepped back down in order to compensate.

The primary reasons for using input and output impedance matching networks are:

1. To obtain desirable component values which reduce the effects of parasitics or component-related losses.
2. To obtain the desired filter impedance behavior with filter center frequency as described in the context of §1.1

### 3 A Simple First-Order Bandpass Filter

One of the most simple first-order bandpass filter constructs is shown here in Figure 14. In principle, the series resonator would suffice for a bandpass filter alone, but this could easily lead to unrealistic component value demands upon  $L_2$  and  $C_2$ . In principle, this problem can be alleviated by including input and output L-matching networks as shown thereby permitting the internal impedance level within the filter to be more arbitrary. Using a single resonator along with simple L-match networks limits this topology to relatively narrow bandwidth applications.



**Figure 14**  $N = 1$  bandpass filter with additional input and output L-matching sections

Assuming that the source impedance is represented by  $R_{source}$  and the load impedance is represented by  $R_{load}$  in the context of Figure 14, capacitance  $C_1$  is based upon a simple L-matching section and given by

$$C_1 = \frac{1}{\omega_c R_{source}} \sqrt{\frac{R_{source}}{R_{internal}} - 1} \quad (21)$$

where  $\omega_c$  is the intended radian center frequency for the passband and  $R_{internal}$  is the internal resistance value intended for the filter. The behavior of  $R_{internal}$  with filter center frequency is a key design choice which is discussed later.

It is straight forward to show that inductor  $L_1$  is given by

$$\begin{aligned} L_1 &= \frac{R_{source}^2 C_1}{1 + (\omega_c R_{source} C_1)^2} \\ &= R_{internal} R_{source} C_1 \end{aligned} \quad (22)$$

Similar results apply to the output L-matching network as

$$C_3 = \frac{1}{\omega_c R_{load}} \sqrt{\frac{R_{load}}{R_{internal}} - 1} \quad (23)$$

$$\begin{aligned} L_3 &= \frac{R_{load}^2 C_3}{1 + (\omega_c R_{load} C_3)^2} \\ &= R_{internal} R_{load} C_3 \end{aligned} \quad (24)$$

Assuming that the desired quality factor for the series resonator is represented by  $Q_{res}$ , the internal resistance level is given by

$$R_{internal} = \frac{\omega_c L_2}{Q_{res}} \quad (25)$$

Based upon (22), (24), and (25), the total series inductance is given by

$$\begin{aligned} L_{series} &= L_1 + L_2 + L_3 \\ &= \frac{R_{internal}}{\omega_c} \sqrt{\frac{R_{source}}{R_{internal}} - 1} + \frac{Q_{res} R_{internal}}{\omega_c} + \frac{R_{internal}}{\omega_c} \sqrt{\frac{R_{load}}{R_{internal}} - 1} \end{aligned} \quad (26)$$

In the usual case where  $R_{source} = R_{load}$ , (26) can be simplified to

$$L_{series} = \frac{2R_{internal}}{\omega_c} \sqrt{\frac{R_{source}}{R_{internal}} - 1} + \frac{Q_{res} R_{internal}}{\omega_c} \quad (27)$$

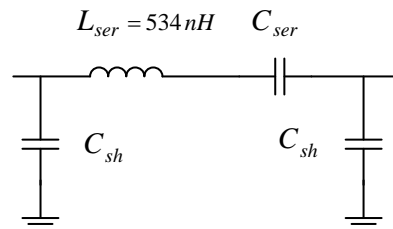
In order to have an implementable tunable filter, only the capacitors in Figure 14 should be adjustable and the series inductance  $L_{series}$  should be fixed across the center frequency tuning range of interest. Consequently, (27) can be used to determine the required behavior for  $R_{internal}$  in order to keep  $L_{series}$  a constant. After some algebraic re-arrangement, (27) can be written as a quadratic in  $R_{internal}$  as

$$R_{internal}^2 \left( \frac{4 + Q_{res}^2}{\omega_c^2} \right) - R_{internal} \left( \frac{2Q_{res} L_{series}}{\omega_c} + \frac{4R_{series}}{\omega_c^2} \right) + L_{series}^2 = 0 \quad (28)$$

Since the design requires that  $L_{series}$  be constant across the entire frequency tuning range, ideally the derivative of (27) with respect to  $\omega_c$  should be zero across the tuning range of interest. No solution exists, however, unless  $R_{internal}$  is allowed to change with center frequency  $\omega_c$ .

### 3.1 A Design Example

Assume that the desired center frequency tuning range is 30 MHz to 90 MHz and  $Q_{res} = 7$  is desired. Under this assumption, choosing  $L_{series} = 533.56$  nH produces the computed  $R_{internal}$  from (28) as shown in Figure 17 with the filter schematic as shown in Figure 15. The capacitance values versus filter center frequency are given in Figure 16.



**Figure 15** First-order bandpass filter solution where  $C_{sh}$  and  $C_{ser}$  vary versus filter center frequency as shown in Figure 16

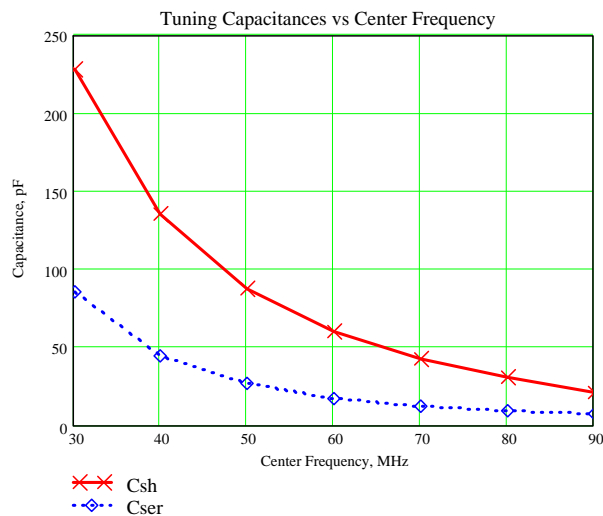


Figure 16  $C_{sh}$  and  $C_{ser}$  for Figure 15

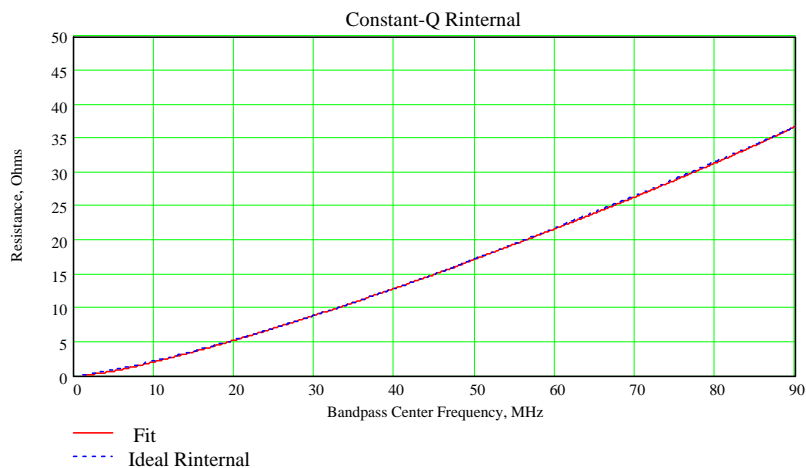
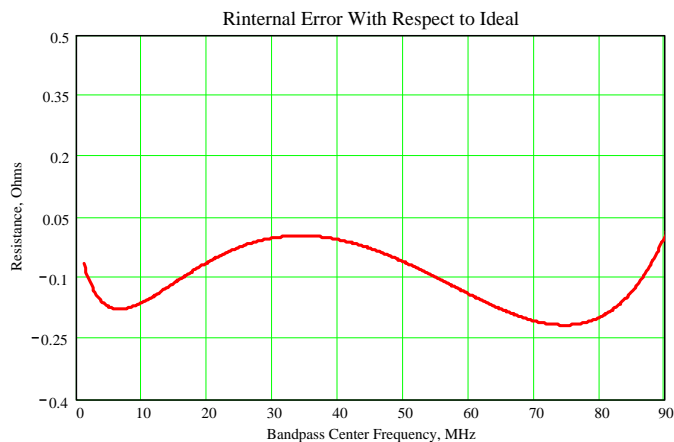


Figure 17 Constant  $Q_{res} (= 7)$  solution to (28) with  $L_{series} = 533.56$  nH

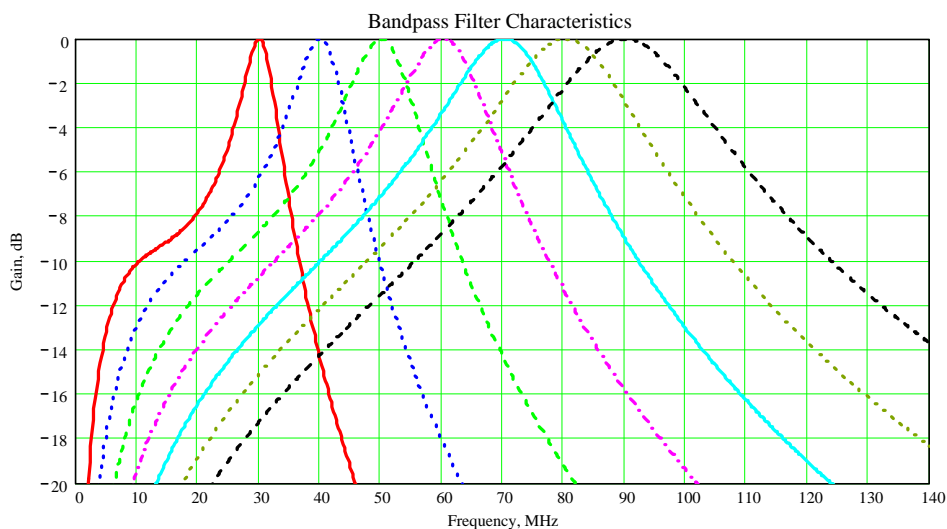
It turns out that choosing

$$R_{internal}(f_{MHz}) = R_d \left( \frac{f_{MHz}}{f_{max\_MHz}} \right)^{1.2916} \tag{29}$$

along with  $R_d = 36.8\Omega$  is an almost ideal solution. The difference between the ideal value for  $R_{internal}$  and (29) is plotted in Figure 18. The resultant filter gain characteristics versus center frequency are shown in Figure 19 where the constant-Q choice results in the filter's bandwidth increasing with center frequency.



**Figure 18** Resistance error of (29) with respect to ideal as computed using (28)



**Figure 19** Filter characteristics for difference center frequencies assuming the design details associated with Figure 17 and Figure 18. Ideal components have been assumed.

### 3.2 An Alternative Configuration- Constant Bandwidth

Motivated by (27), other possibilities for the  $R_{internal}(f)$  function can be also considered. In the VHF frequency range, the inductor-Q frequently increases with frequency thereby making it attractive to consider making the tunable bandpass filter constant-bandwidth in nature, rather than constant-Q. Taking this approach, the quantity  $\omega_c / Q_{res}$  in (27) should remain a fixed (radian-) bandwidth represented here by  $B$ . Substituting this into (27) changes the design equation for  $R_{internal}$  to



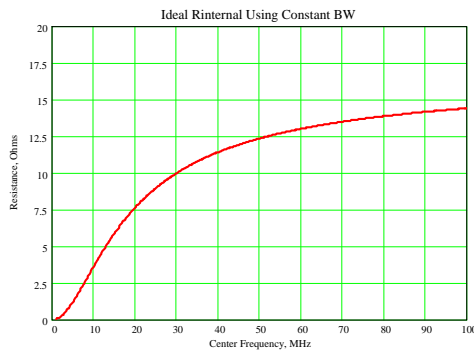
$$L_{series} = \frac{2R_{internal}}{\omega_c} \sqrt{\frac{R_{source}}{R_{internal}} - 1} + \frac{R_{internal}}{B} \tag{30}$$

which then leads to

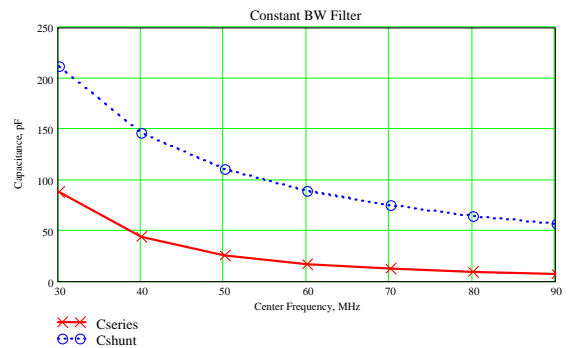
$$R_{internal}^2 \left( \frac{1}{B^2} + \frac{4}{\omega_c^2} \right) - R_{internal} \left( \frac{2L_{series}}{B} + \frac{4R_{source}}{\omega_c^2} \right) + L_{series}^2 = 0 \tag{31}$$

Other variations of this approach are of course possible. For example, the filter bandwidth could be allowed to increase at some specified rate with increasing center frequency and (29) subsequently modified.

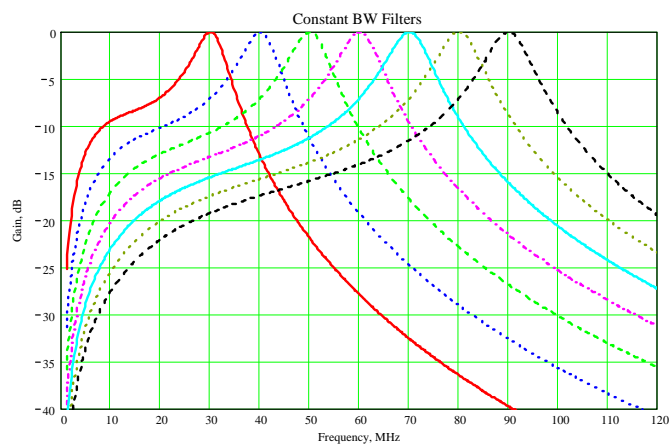
For the constant filter bandwidth case (tuning from 30 MHz through 90 MHz) with a fixed filter bandwidth of 5 MHz, the ideal inductor value is about 533 nH and the corresponding series and shunt capacitor values given as shown in Figure 21. The resultant filter responses versus center frequency are shown in Figure 22 for the ideal component case. The circuit topology is identical to that shown in Figure 15 but the tuning capacitor values are varied differently with frequency.



**Figure 20** Ideal  $R_{internal}$  for a constant filter bandwidth of 5 MHz



**Figure 21** Shunt and series filter capacitances associated with Figure 20



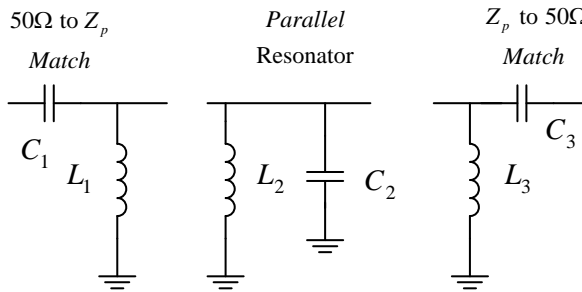
**Figure 22** Constant filter bandwidth characteristics associated with Figure 20 and the design approach suggested in this section. Infinite component-Q's assumed.

## 4 1<sup>st</sup>-Order Step-Up Impedance Configuration

The internal resistance levels shown in Figure 20 are quite low compared to the on-resistance of FET switches in the case of a design for RFICs. The FET switch resistance consequently plays a serious role in dictating the filter insertion loss. The high-impedance equivalent to Figure 14 is shown here in Figure 23. This configuration is also attractive in that every internal node has intentional shunt-capacitance to ground whereas this is not quite as true with the original construct in Figure 14.

The RF switches are involved with all of the capacitors of course while the shunt inductor (parallel combination of  $L_1$ ,  $L_2$ , and  $L_3$ ) is fixed.

One notable down-side of this configuration is that the impedance level is stepped-up around the parallel resonator so the voltage-swing of any in-band signals will also be increased. Consequently, the insertion loss of this filter may be lower than that of Figure 14 but its 3<sup>rd</sup>-order intercept point may be poorer than that of Figure 14. The upper stopband attenuation will also be poorer due to the input/output capacitive coupling used.



**Figure 23** Dual first-order bandpass filter to Figure 14

Based upon calculations quite similar to those used earlier in §3 and §3.2, the component values in Figure 23 are given by

$$C_1 = \frac{1}{\omega_c R_{source}} \sqrt{\frac{R_{source}}{R_{internal} - R_{source}}} \quad (32)$$

$$L_1 = L_3 = \frac{1 + (\omega_c R_{source} C_1)^2}{\omega_c^2 C_1} = R_{internal} R_{source} C_1 \quad (33)$$

where the source and load resistances have again been assumed to be equal. The total shunt inductance is given by

$$L_p = \left( \frac{1}{L_1} + \frac{1}{L_2} + \frac{1}{L_3} \right)^{-1} = \frac{L_1 L_2}{2L_2 + L_1} \quad (34)$$

By definition,

$$L_2 = \frac{R_{internal}}{\omega_c Q_{res}} \quad (35)$$

Putting (34) together with (33) and (35) produces the result

$$L_p = \frac{R_{internal}}{\omega_c Q_{res}} \frac{\sqrt{\frac{R_{source}}{R_{internal} - R_{source}}}}{\frac{2}{Q_{res}} + \sqrt{\frac{R_{source}}{R_{internal} - R_{source}}}} \quad (36)$$

After some algebraic manipulation, (36) can be recast as a quadratic in  $R_{internal}$  as

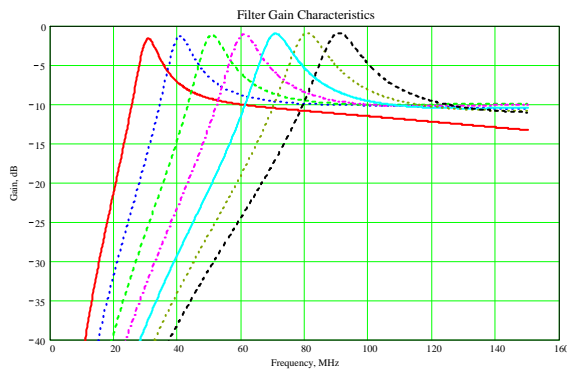
$$R_{internal}^2 - R_{internal} \left( 2\omega_c L_p Q_{res} + \frac{4\omega_c^2 L_p^2}{R_{source}} \right) + (\omega_c L_p)^2 \left( Q_{res}^2 + \frac{4}{R_{source}} \right) = 0 \quad (37)$$

It is convenient to parameterize the desired filter-Q as

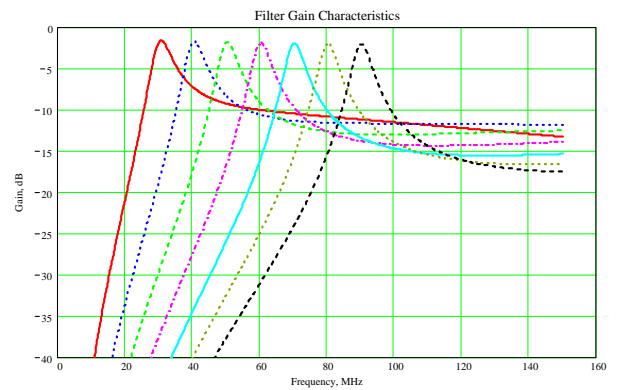
$$Q_{res}(f) = Q_{fil} \left( \frac{f}{f_{min}} \right)^\gamma \quad (38)$$

where  $\gamma = 0$  corresponds to a constant-Q filter design and  $\gamma = 1$  corresponds to a constant-bandwidth filter design.

It turns out that the choice for the total inductance  $L_p$  is fairly non-critical. The filter's upper stopband performance is, however, quite poor unless an overly large inductance value is assumed (which would lead to other issues). As originally expected though, the filter's insertion loss is driven almost entirely by inductor-Q whereas RF switch resistance effects are almost negligible. Filter behavior for a constant-Q and constant-bandwidth design are shown in Figure 24 and Figure 25 respectively.



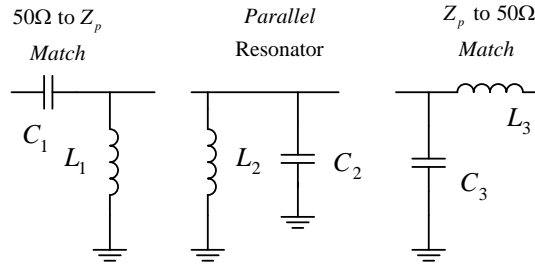
**Figure 24** Filter design characteristics for a constant-Q design ( $\gamma = 0$ ) assuming RF switch on-resistance of  $1\Omega$ , minimum inductor-Q of 80, filter-Q of 8, and  $L_p = 120$  nH. Although the lower stopband performance is excellent because of the input & output capacitive coupling, the upper stopband performance is quite poor.



**Figure 25** Filter design identical to Figure 24 except that a constant bandwidth design is employed ( $\gamma = 1$ )

### 4.1 Improving Upper Stopband Attenuation

The only way to stay with a single parallel resonator and improve the upper stopband performance markedly is to alternate the impedance-matching type between the input and output as shown in Figure 26.



**Figure 26** Single parallel resonator with alternating highpass / lowpass input/output impedance matching

Since all of the inductors must be fixed values (including  $L_3$ ), inductor  $L_3$  sets the internal resistance level for the filter. Inductor  $L_3$  must be selected such that the parallel combination of  $L_1$  and  $L_2$  remains constant over the tuning range of interest.

Given a value for  $L_3$ ,

$$R_{\text{internal}} = R_{\text{source}} + \frac{(\omega_c L_3)^2}{R_{\text{source}}} \quad (39)$$

and

$$C_3 = \frac{L_3}{R_{\text{source}}^2 + (\omega_c L_3)^2} \quad (40)$$

Given  $R_{\text{internal}}$  from (39), values for  $C_1$  and  $L_1$  are determined in the same way as done earlier as

$$C_1 = \frac{1}{\omega_c R_{\text{source}}} \sqrt{\frac{R_{\text{source}}}{R_{\text{internal}} - R_{\text{source}}}} \quad (41)$$

$$L_1 = \frac{R_{\text{internal}}}{\omega_c} \sqrt{\frac{R_{\text{source}}}{R_{\text{internal}} - R_{\text{source}}}} \quad (42)$$

Resonator values are straight forward as

$$L_2 = \frac{R_{\text{internal}}}{Q_{\text{res}} \omega_c} \quad (43)$$

$$C_2 = \frac{Q_{\text{res}}}{\omega_c R_{\text{internal}}}$$

The parallel combination of  $L_1$  and  $L_2$ , denoted here by  $L_p$ , must be constant as stated earlier where

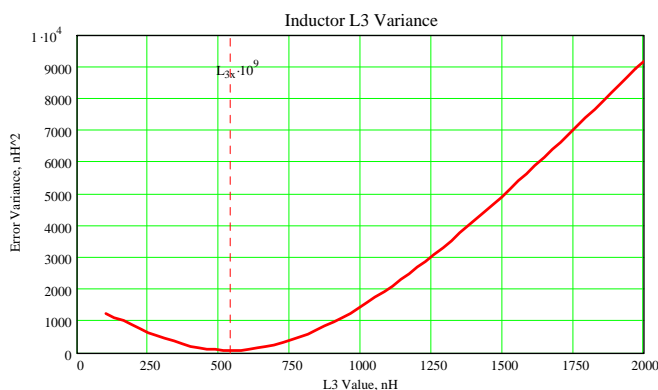
$$L_p = \frac{L_1 L_2}{L_1 + L_2} \quad (44)$$

Using (42) and (43) in (44) produces

$$L_p = \frac{\sqrt{\frac{R_{source}}{R_{internal} - R_{source}} \frac{R_{internal}}{\omega_c Q_{res}}}}{\sqrt{\frac{R_{source}}{R_{internal} - R_{source}} + \frac{1}{Q_{res}}}} \quad (45)$$

Equation (38) can be used for the resonator's Q value once again.

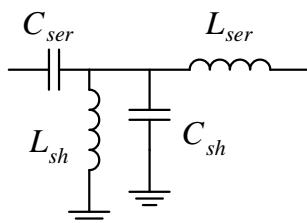
The design proceeds by first picking a value for  $L_3$  which minimizes the variance of  $L_p$  over the desired tuning range for the filter. For the case where  $Q_{fil}$  and  $\gamma$  equal 5 and 0.75 respectively in (38) with a filter tuning range of 30 MHz to 90 MHz, an optimal value for  $L_3$  is about 540 nH as shown in Figure 27.



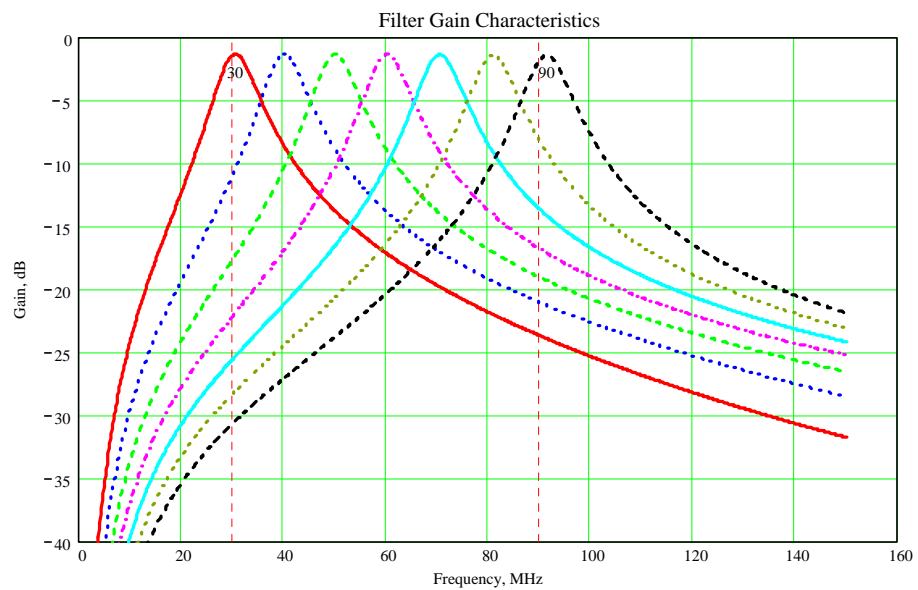
**Figure 27** Brute-force optimization for inductor  $L_3$

The other component values are computed using the previous equations while assuming  $L_3 = 540$  nH. The resultant filter gain characteristics at multiples of 10 MHz are shown in Figure 29. Insertion loss is quite reasonable even with RF switch on-resistance and finite inductor-Q included.

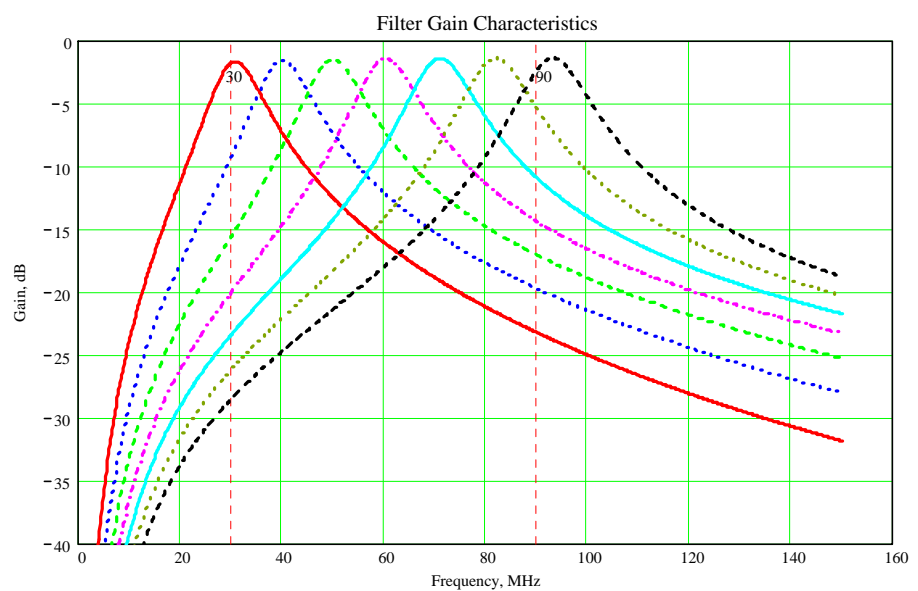
If the  $\gamma$  value is changed, the optimum value for  $L_3$  also changes. Optimum values are 360 nH and 250 nH for  $\gamma$  values of 0.50 and 0.25 respectively. Filter gain characteristics for these two cases are shown in Figure 30 and Figure 31. The filter topology is the same for all of these cases as given in Figure 28. Depending upon the case, the tuning capacitances  $C_{ser}$  and  $C_{sh}$  are adjusted versus frequency as shown in Figure 32, Figure 33, and Figure 34.



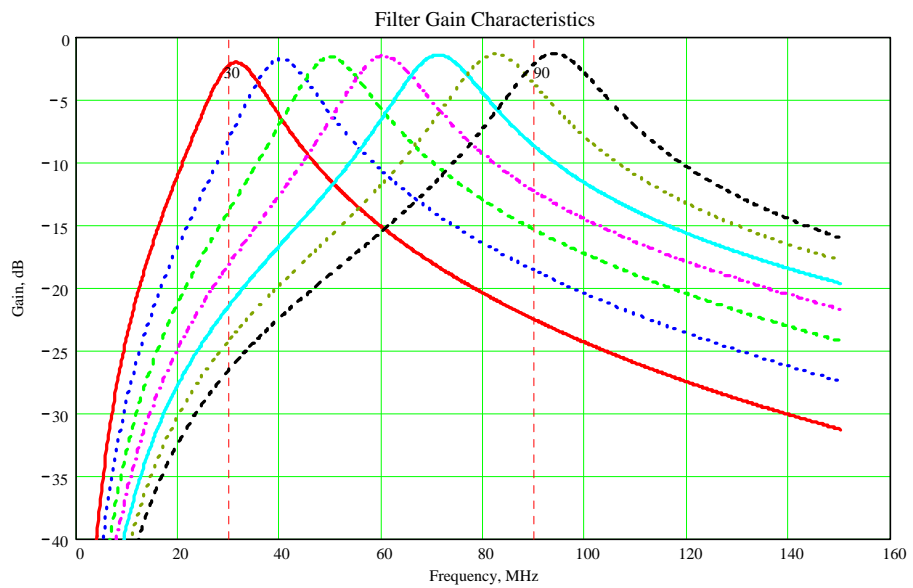
**Figure 28** Filter topology for this group of solutions



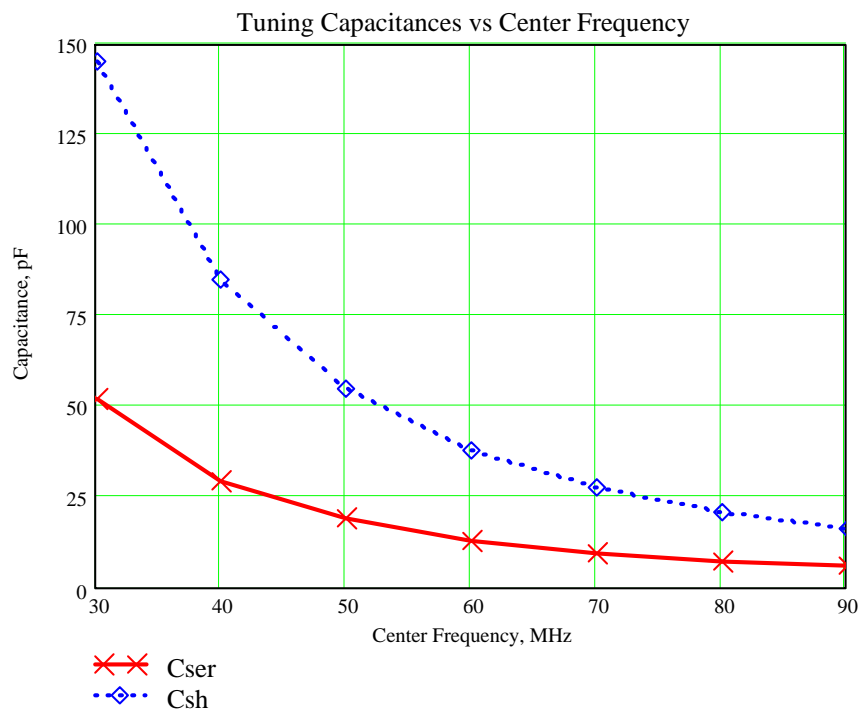
**Figure 29** Filter gain characteristics assuming a nominal inductor-Q of 80,  $\gamma = 0.75$ , and RF switch on-resistance of  $1\Omega$ . Optimum value for  $L_{ser} = L_3$  is about 540 nH and  $L_{sh} = 185.6$  nH. See Figure 32 for tuning capacitance values versus filter center frequency.



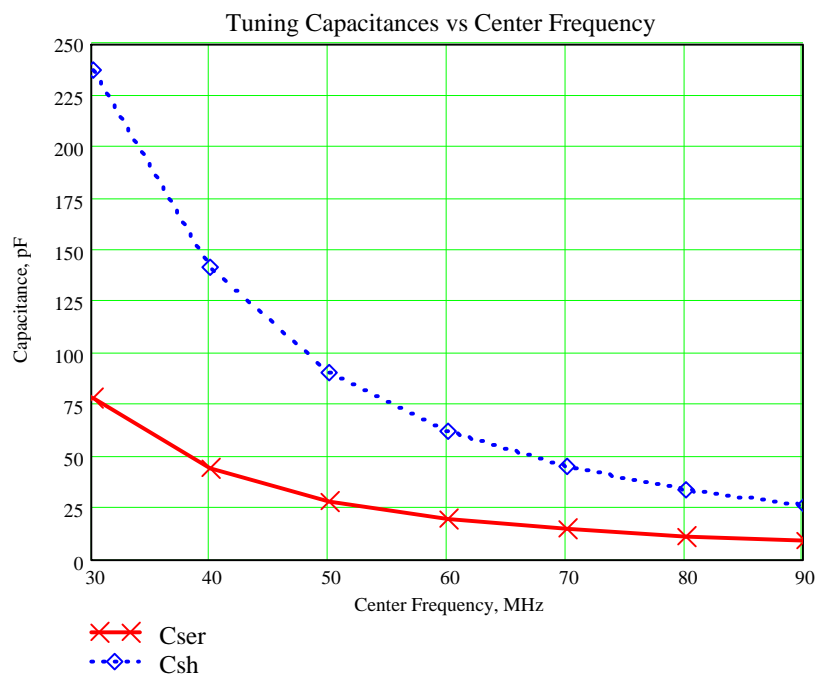
**Figure 30** Filter gain characteristics assuming a nominal inductor-Q of 80,  $\gamma = 0.50$ , and RF switch on-resistance of  $1\Omega$ . Optimum value for  $L_{ser} = L_3$  is about 360 nH and  $L_{sh} = 111.7$  nH. See Figure 33 for tuning capacitance values versus filter center frequency.



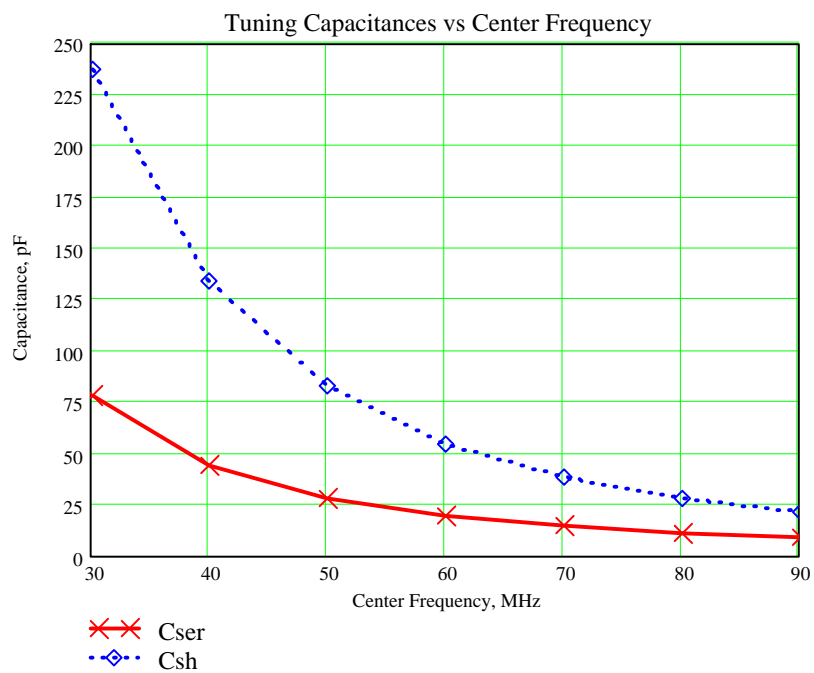
**Figure 31** Filter gain characteristics assuming a nominal inductor-Q of 80,  $\gamma = 0.25$ , and RF switch on-resistance of  $1\Omega$ . Optimum value for  $L_{ser} = L_3$  is about 250 nH and  $L_{sh} = 122.6$  nH.



**Figure 32** Tuning capacitance values versus filter center frequency pertaining to Figure 28 and Figure 29



**Figure 33** Tuning capacitance values versus filter center frequency pertaining to Figure 28 and Figure 30

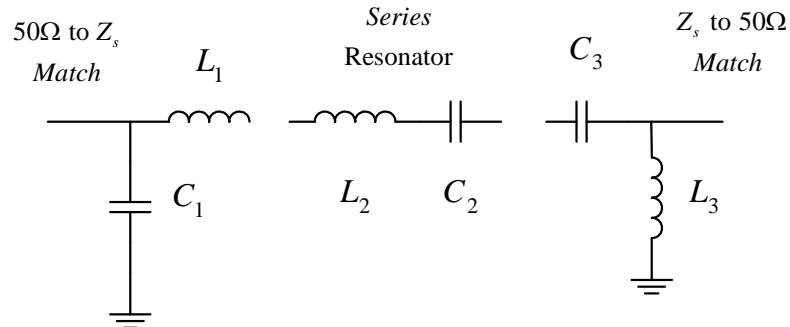


**Figure 34** Tuning capacitance values versus filter center frequency pertaining to Figure 28 and Figure 31



## 5 1<sup>st</sup>-Order Step-Down Configuration Revisited

The original step-down filter configuration discussed in §3 used the same style of lowpass matching sections at the input and the output. In this section, a highpass matching section is used at the output port instead as shown in Figure 35. Once again, fixed inductor  $L_3$  determines the behavior of  $R_{internal}$  versus the filter's center frequency.



**Figure 35** Step-down filter configuration with a highpass matching section at the output port

The filter's internal resistance level is given by

$$R_{internal} = \frac{(\omega_c L_3)^2 R_{load}}{R_{load}^2 + (\omega_c L_3)^2} \quad (46)$$

The other design equations are

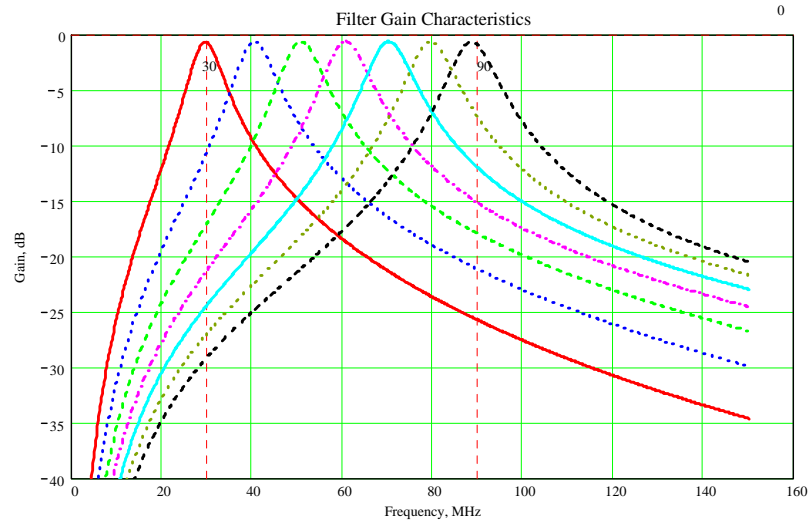
$$\begin{aligned} C_3 &= \frac{L_3}{R_{internal} R_{load}} \\ C_2 &= \frac{1}{\omega_c Q_{res} R_{internal}} \\ C_1 &= \frac{1}{\omega_c R_{source}} \sqrt{\frac{R_{source}}{R_{internal}} - 1} \end{aligned} \quad (47)$$

and

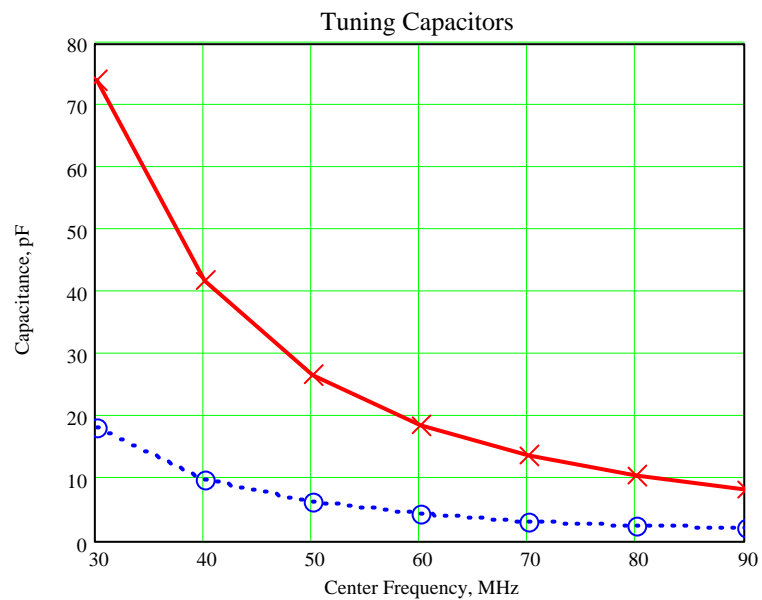
$$\begin{aligned} L_1 &= R_{internal} R_{source} C_1 \\ L_2 &= \frac{Q_{res} R_{internal}}{\omega_c} \end{aligned} \quad (48)$$

For proper filter performance,  $L_3$  needs to be selected such that  $L_p = L_1 + L_2$  is as constant across the intended center-frequency tuning range as possible.

Choosing  $Q_{fil} = 8$  and  $\gamma = 0.75$  in (38) and  $L_3 = 380$  nH results in the filter behavior shown in Figure 36 using the tuning capacitor values shown in Figure 37.



**Figure 36** Filter gain characteristics assuming a nominal inductor-Q of 80,  $Q_{fill} = 8$ ,  $\gamma = 0.75$ , and RF switch on-resistance of  $1\Omega$ . Optimum value for  $L_3$  is about 380 nH. The filter’s insertion loss is unexpectedly low and stopband performance very good on both sides.



**Figure 37** Tuning capacitor values for Figure 36

## 6 Summary of 1<sup>st</sup>-Order Bandpass Filter Design

A variety of filter configurations have been considered, both in topology as well as variants spanning from constant-Q to constant-bandwidth filters using parameter  $\gamma$ . The different filter cases considered are summarized in Table 3.

**Table 3** Summary of 1<sup>st</sup>-Order Bandpass Filters Considered

Figure	Input Match	Output Match	Resonator	Behavior	General Performance
Figure 14	LP	LP	Series	Constant-Q	
Figure 22	“	“	“	Constant-BW	
Figure 24	HP	HP	Parallel	Constant-Q	Poor
Figure 25	“	“	“	Constant-BW	Poor
Figure 29 – Figure 31	HP	LP	“	Adjustable	Good
Figure 36	LP	HP	Series	Adjustable	Good

### Summary points:

- Making use of alternative  $R_{internal}$  functions as done in §3.2 is very attractive for having tighter bandwidth control versus tuned center frequency.
- The filter design discussed in §0 does entail one additional inductor, but the nearly symmetric upper and lower stopband attenuation performance is most appealing.
- The last filter topology visited in §5 exhibits an unexpected low insertion loss along with a very good bandpass characteristic and therefore deserves additional consideration.
- Keeping the number of transmission zeros at zero frequency and  $\infty$  frequency balanced helps to preserve good overall stopband performance.

## 7 A Real World Design Example

The preceding design approaches leave many options on the table, even for a first-order bandpass filter! Aside from the more obvious cases like Figure 24 in §4 where the upper stopband is more or less lost, a number of the results look fairly attractive for real-world use.

In general, it is difficult to uniformly obtain more than 20 dB of 2<sup>nd</sup> harmonic suppression over an octave tuning range without the filter insertion loss becoming excessive. If the objective is more on the order of 40 dB of suppression, a cascade of 1<sup>st</sup> order sections or the  $N = 2$  filters discussed in Part II will be a much better choice.

To illustrate a real world design example more fully, the results shown in Figure 29 and Figure 32 will be looked at in greater detail here. This filter design provides between roughly 15 dB and 22 dB of 2<sup>nd</sup> harmonic suppression with good stopband symmetry. The insertion loss shown is due entirely to inductor-Q and assumed varactor-Q or switch-related losses.

Assume that a tunable filter is required to cover from 100 MHz through 200 MHz and it is determined that a filter-Q of 5 at 100 MHz provides sufficient selectivity. The choice for  $\gamma$  is 0.75. The optimum shunt inductance value is given by (45) as about 28.7 nH whereas the optimal choice for  $L_{ser}$  is about 200 nH. Given these choices, the  $C_{ser}$  and  $C_{sh}$  capacitance values should be varied with filter center frequency as shown in Figure 39. The resultant frequency response is shown in Figure 40.

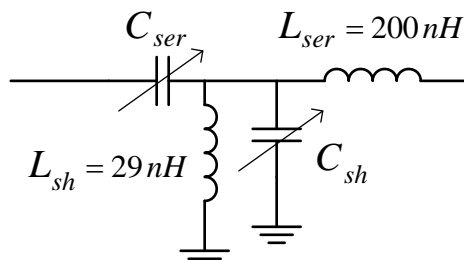


Figure 38 Filter topology for this example

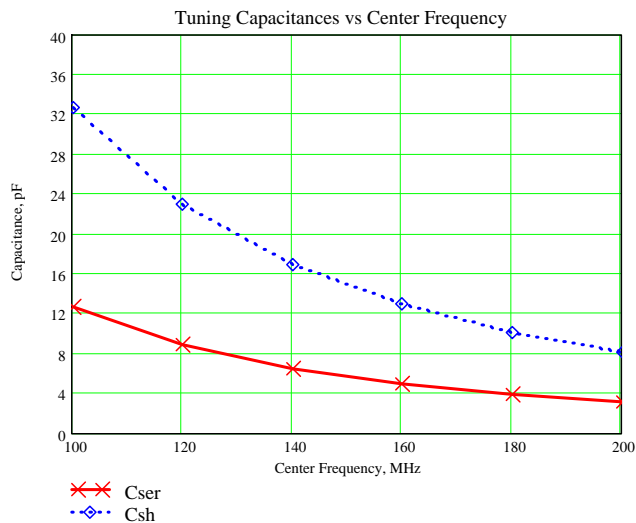
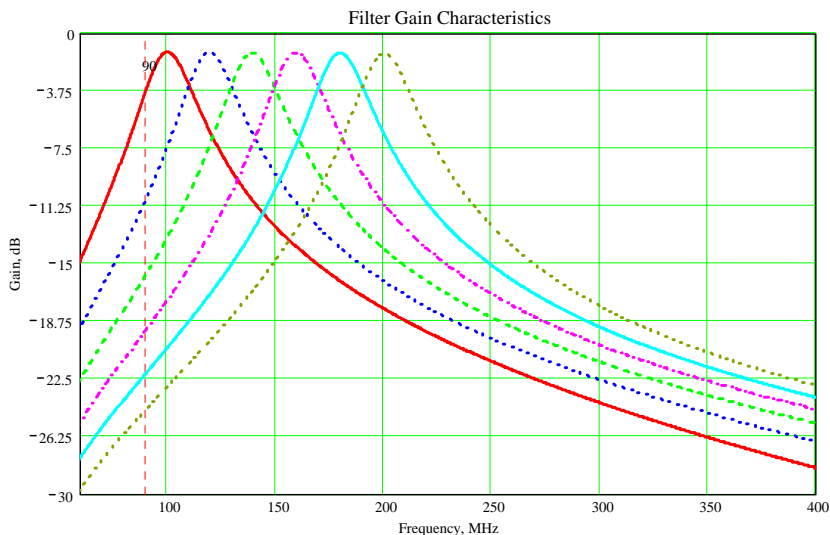


Figure 39 Optimal values for tuning capacitors in Figure 38

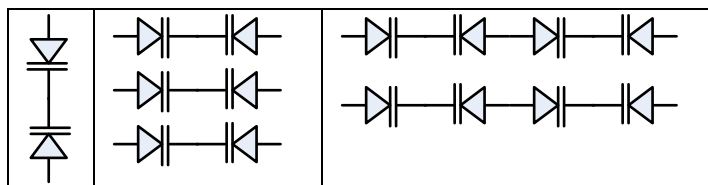


**Figure 40** Associated frequency response for several filter center frequencies situated between 100 MHz and 200 MHz

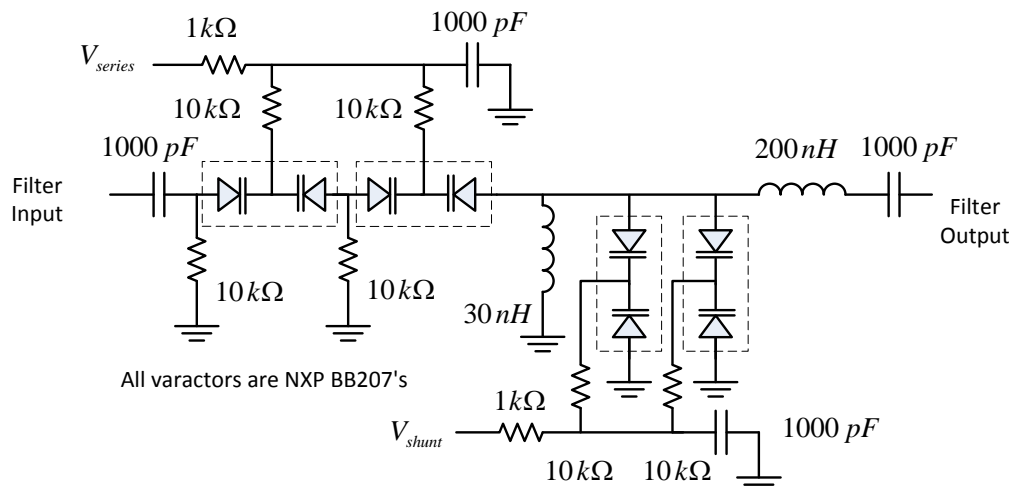
For the tunable capacitors, it is generally easier to use varactor diodes than to use a bank of switched capacitors. Finding RF switches with sufficiently low on-resistance can be a challenging issue, or PIN diodes can be used if the high current drain involved can be tolerated.

If varactors are used for the tunable capacitances, it is always best to use combinations of back-to-back varactors because this substantially improves linearity. Using series and parallel combinations of such varactor-pairs can be helpful for realizing a wide range of capacitance values while only requiring one varactor type as suggested in Table 4.

**Table 4** Example series and parallel combinations of varactor diodes



For a prototype filter, BB207 common-cathode varactors are readily available. A single varactor is adjustable from about 17 pF to 80 pF using a bias voltage from 15V down to 1V. Tuning at the upper-end of the tuning range may be somewhat compromised, but certainly adequate for a first prototype investigation. The more detailed filter schematic is shown in Figure 41.



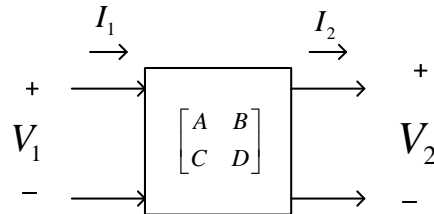
**Figure 41** Detailed schematic for the 100 MHz to 200 MHz tunable 1<sup>st</sup>-order bandpass filter

## 7.1 Filter Alignment Possibilities

A variety of means can be used to align the filter across frequency when varactor tuning is assumed. The first means is to simply build a table of values in which  $C_{sh}$  is stepped by adjusting and  $C_{ser}$  is varied at each step (by adjusting  $V_{series}$ ) to minimize the insertion loss. Since both adjustable capacitance values affect the center frequency, the third entry in the table is the resultant center frequency once the insertion loss has been minimized by adjusting  $V_{series}$ . This table can be used to interpolate the required tuning voltages for any center frequency across the band.

## 8 Filter Analysis Method

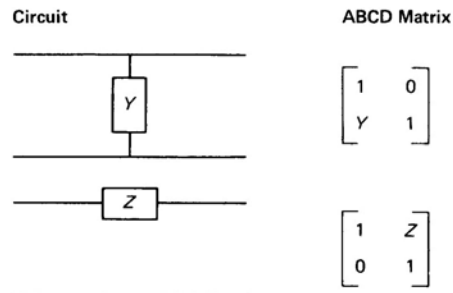
A wide range of different software tools could be used to analyze the different filter schematics presented in this paper. The adopted approach, however, is based upon  $ABCD$  matrices [2] using MATLAB. A basic  $ABCD$  linear system is shown in Figure 42 with



**Figure 42**  $ABCD$  matrix definition

$$\begin{aligned} V_1 &= AV_2 + BI_2 \\ I_1 &= CV_2 + DI_2 \end{aligned} \quad (49)$$

This arrangement makes it very easy to cascade circuit elements which can be drawn in a ladder arrangement. The  $ABCD$  matrix for a shunt admittance and a series impedance are shown in Figure 43.



**Figure 43**  $ABCD$  matrices for shunt and series elements

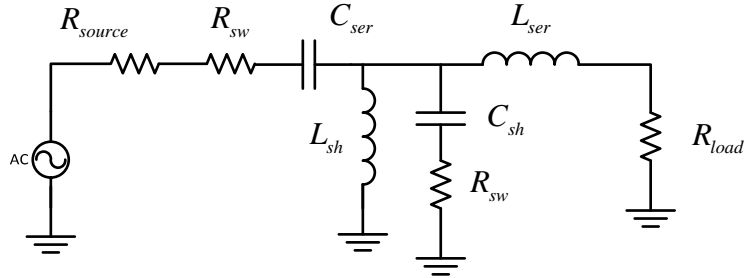
The input impedance associated with (49) when the load is a simple resistance  $R_{load}$  is given by

$$\begin{aligned} Z_{in} &= \frac{V_1}{I_1} = \frac{AV_2 + BI_2}{CV_2 + DI_2} = \frac{AV_2 + B(V_2 / R_{load})}{CV_2 + D(V_2 / R_{load})} \\ &= \frac{AR_{load} + B}{CR_{load} + D} \end{aligned} \quad (50)$$

Similarly, the output to input voltage gain is given by

$$\begin{aligned} G_v &= \frac{V_2}{V_1} = \frac{V_2}{AV_2 + BI_2} = \frac{V_2}{AV_2 + B(V_2 / R_{load})} \\ &= \frac{R_{load}}{AR_{load} + B} \end{aligned} \quad (51)$$

The filter configuration shown in Figure 28 is repeated here switched-capacitor switch resistances and finite inductor-Q in Figure 44. The  $ABCD$  matrix cascade for this schematic is given by



**Figure 44** Filter schematic of Figure 28 including capacitor-switch resistances along with source and load resistances

$$\begin{aligned}
 ABCD(s) = & \begin{bmatrix} 1 & \left( R_{sw} + \frac{1}{sC_{ser}} \right) \\ 0 & 1 \end{bmatrix} \times \begin{bmatrix} 1 & 0 \\ \frac{1}{sL_{sh} \left( 1 - \frac{j}{Q_{ind}} \right)} & 1 \end{bmatrix} \times \\
 & \begin{bmatrix} 1 & 0 \\ \frac{1}{R_{sw} + \frac{1}{sC_{sh}}} & 1 \end{bmatrix} \times \begin{bmatrix} 1 & sL_{ser} \left( 1 - \frac{j}{Q_{ind}} \right) \\ 0 & 1 \end{bmatrix}
 \end{aligned} \tag{52}$$

where  $s$  is the normal Heaviside operator and  $j = \sqrt{-1}$ . Note that finite inductor-Q has been included by way of  $Q_{ind}$ .

To analyze the filter described by (52), all of the inductance values remain constant. Values for  $C_{ser}$  and  $C_{sh}$  are determined based upon the desired center frequency of the filter using (41) for  $C_{ser}$  and the sum of (43) and (40) for  $C_{sh}$ . The frequency response of the filter is obtained by computing the  $ABCD$  matrix (52) at each sweep-frequency of interest and using (53) to compute the (complex) input reflection coefficient  $S_{11}$  and using (54) to compute the power-gain  $S_{21}$ .

$$S_{11} = \frac{AR_{load} + B - CR_{source}R_{load} - DR_{source}}{d} \tag{53}$$

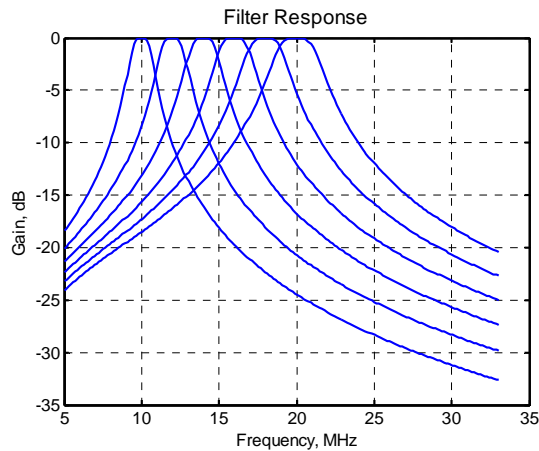
$$S_{21} = \frac{2\sqrt{R_{source}R_{load}}}{d} \tag{54}$$

$$d = AR_{load} + B + CR_{source}R_{load} + DR_{source} \tag{55}$$



## 9 Looking Ahead

Generally speaking, filter passband flatness dictates that the filter order necessarily be increased to at least two. In Part II of this series, details will be presented for nearly symmetric wide-tuning range 2<sup>nd</sup>-order LC bandpass filters. Well behaved tuning ranges in excess of an octave can be achieved.



**Figure 45** Tunable filter frequency response for different center frequencies for 2<sup>nd</sup>-order LC bandpass filters

## 10 References

1. Arthur Williams and Fred Taylor, *Electronic Filter Design Handbook*, 4<sup>th</sup> ed., McGraw-Hill, 2006.
2. W. Alan Davis, *Microwave Semiconductor Circuit Design*, Van Nostrand Reinhold, 1984.